AGU PUBLICATIONS

Radio Science

RESEARCH ARTICLE
10.1002/2014RS005601

Key Points:
- Low VHF has favorable short-range characteristics and low signal distortion
- Penetration through many layers of building walls is possible at low VHF
- Novel miniaturized VHF antennas with reasonable performance have been designed

Correspondence to:
F. T. Dagefu,
DFikadu@gmail.com

Citation:
Dagefu, F. T., J. Choi, M. Sheikhsofla, B. M. Sadler, and K. Sarabandi (2015), Performance assessment of lower VHF band for short-range communication and geolocation applications, *Radio Sci.*, *50*, 443–452, doi:10.1002/2014RS005601.

Received 23 OCT 2014
Accepted 14 APR 2015
Accepted article online 21 APR 2015
Published online 25 MAY 2015

Performance assessment of lower VHF band for short-range communication and geolocation applications

Fikadu T. Dagefu[1], Jihun Choi[2], Morteza Sheikhsofla[2], Brian M. Sadler[1], and Kamal Sarabandi[2]

[1]U.S. Army Research Laboratory, Adelphi, Maryland, USA, [2]Department of Electrical Engineering and Computer Science, University of Michigan, Ann Arbor, Michigan, USA

Abstract The focus of this paper is to characterize near-ground wave propagation in the lower very high frequency (VHF) band and to assess advantages that this frequency band offers for reliable short-range low-data rate communications and geolocation applications in highly cluttered environments as compared to conventional systems in the microwave range. With the advent of palm-sized miniaturized VHF antennas, interest in low-power and low-frequency communication links is increasing because (1) channel complexity is far less in this frequency band compared to higher frequencies and (2) significant signal penetration through/over obstacles is possible at this frequency. In this paper, we quantify the excess path loss and small-scale fading at the lower VHF and the 2.4 GHz bands based on short-range measurements in various environments. We consider indoor-to-indoor, outdoor-to-indoor, and non-line-of-sight outdoor measurements and compare the results with measurements at higher frequencies which are used in conventional systems (i.e., 2.4 GHz). Propagation measurements at the lower VHF band are carried out by using an electrically small antenna to assess the possibility of achieving a miniaturized, mobile system for near-ground communication. For each measurement scenario considered, path loss and small-scale fading are characterized after calibrating the differences in the systems used for measurements at different frequencies, including variations in antenna performance.

1. Introduction

Reliable wireless communication is vital for many civilian and military applications. In complex propagation scenarios such as caves, complex terrain, and indoor and urban environments, signal attenuation and multipath impose stringent conditions on power and signal processing. This is especially true at frequency bands where conventional communication systems operate (i.e., UHF and microwave bands). One application of interest is achieving a reliable communication link among an ensemble of small aerial and/or ground robotic platforms deployed in such environments to enhance tactical situational awareness. Radio communication presents complex challenges for the small robotic platforms because important wireless infrastructures, such as base stations with predetermined positions, are typically absent and high transmit power is not available. Much effort has been devoted over many decades to design modulation schemes appropriate for different communication bands to overcome challenges introduced by the communication channel and factors such as noise and interference.

In general, it is understood that channel complexity is far less at lower frequencies for two reasons. First, significant signal penetration through/over obstacles is possible. Second, reflection, scattering, and diffraction phenomenon is less significant than what is encountered at UHF and higher bands. The severe signal fluctuations and intermittent signal dropoff that are unavoidable at higher frequencies are significantly reduced at the HF and lower VHF bands due to reduced reflection and scattering. It should be mentioned, however, that the multipath effect is the main source of connectivity between a transmitter and a receiver in a complex environment at higher frequencies, where the direct path signal is extremely weak. On the other hand, at lower frequencies, the size of conventional antennas is very large, making application of such systems limited to stationary nodes or, in the case of mobile nodes, the transmit power has to be high enough to compensate for the poor efficiency of the antennas.

With the advent of miniaturized HF and lower VHF antennas having a moderate gain [*Oh et al.*, 2013; *Choi and Sarabandi*, 2014], interest in low-power HF and VHF communication links is increasing. In order to quantitatively study the advantages of an ad hoc wireless system at the lower VHF band for short-range communications and geolocation applications in cluttered environments, accurate field coverage, path loss, and

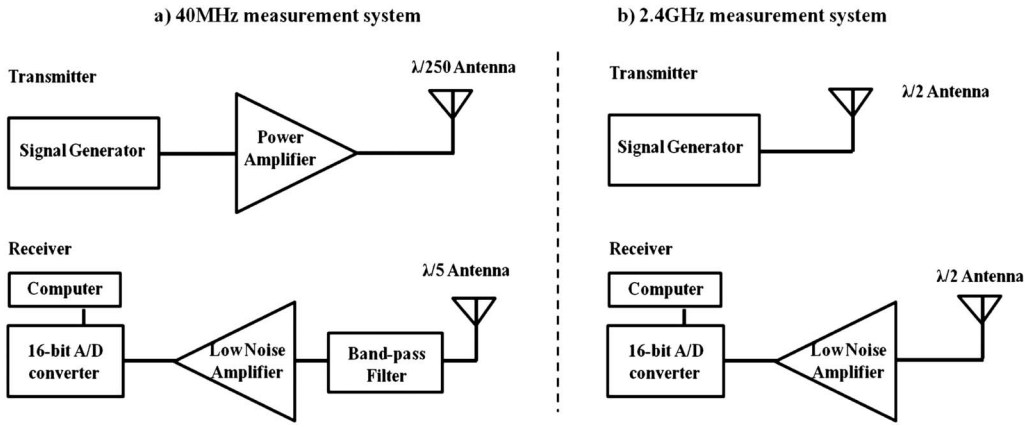

Figure 1. Transmit and receive system diagram for the (a) 40 MHz measurements and the (b) 2.4 GHz measurements are given.

small-scale fading measurements in representative complex propagation scenarios are needed. Although there has been significant work done to study propagation at different frequency bands including microwave, UHF, and VHF bands [*Hampton et al.*, 2006; *Andrusenko et al.*, 2008; *Ali-Rantala et al.*, 2003; *Ruthroff*, 1971; *Liao and Sarabandi*, 2005; *Pugh et al.*, 2006; *Holloway et al.*, 1997; *LaFortune and Lecours*, 1990; *Dagefu et al.*, 2013; *Dagefu and Sarabandi*, 2011], quantitative studies of the short-range low-power wireless channel in lower frequency bands (e.g., HF/lower VHF bands) are not available.

In this paper, propagation measurements in complex indoor/outdoor scenarios are utilized to quantitatively study the advantages of a radio link in the lower VHF band as compared to conventional higher frequencies (e.g., 2.4 GHz). In section 2, we describe the measurement system including the design and characterization of an extremely small antenna operating in the lower VHF band, which is integrated with the measurement system. The measurement scenarios are presented in section 3. In section 4, the propagation measurement

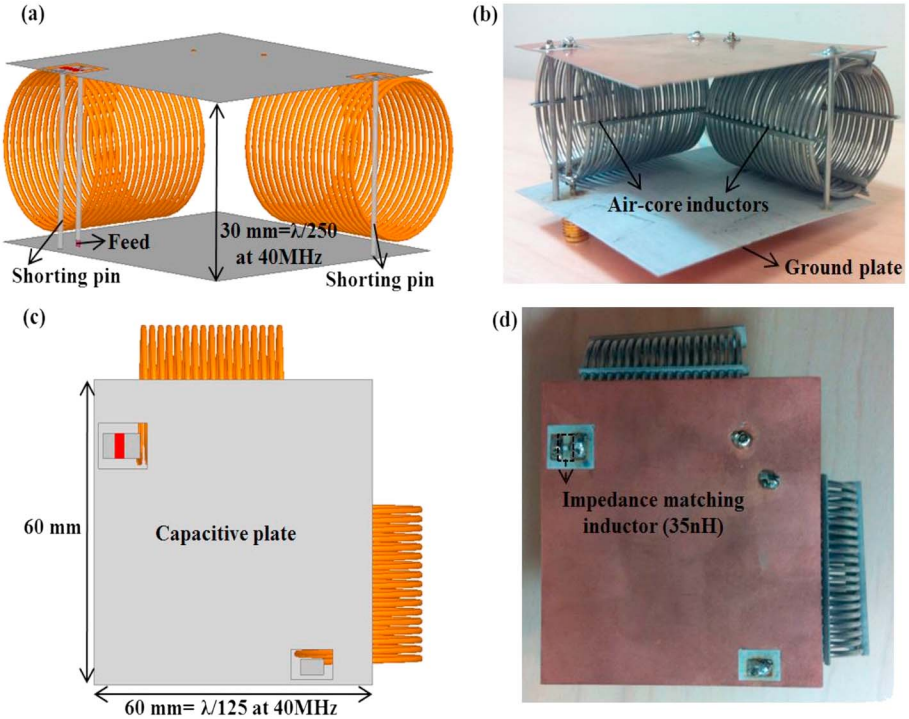

Figure 2. (a and c) The optimized dimensions of the extremely miniaturized antenna incorporating air core inductors are shown. The (b) side view and (d) top view of the fabricated antenna are shown.

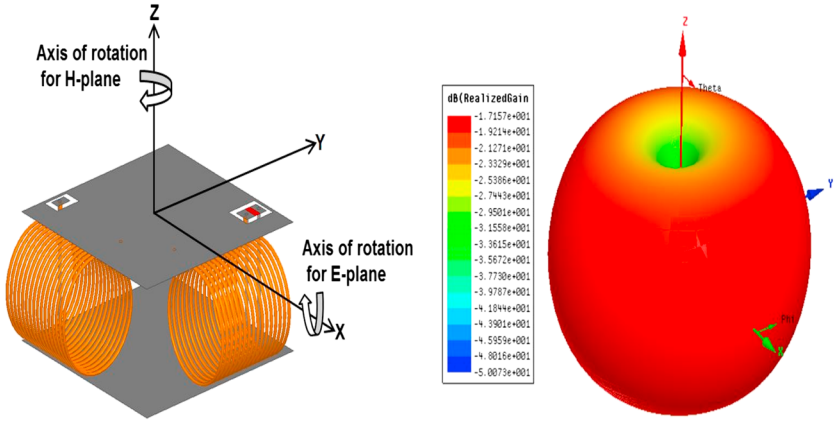

Figure 3. Three-dimensional radiation pattern (E_θ) of the extremely miniaturized low-VHF antenna.

results are discussed. Path loss and small-scale fading comparison at 40 MHz and 2.4 GHz for various non-line-of-sight (NLOS) scenarios are also presented.

2. Measurement System

2.1. 40 MHz Receiver Hardware

A highly sensitive receive circuit was designed and fabricated to accurately measure propagation at the HF and lower VHF band. The receiver system consists of a low-power 16 bit, two-channel analog to digital (A/D) converter which also has a wide dynamic range. The A/D converter has a maximum available sampling rate of 80e6 Samples/sec. A narrow-band, low-insertion loss band-pass filter along with a 40 dB low-noise amplifier is also used to enhance/suppress the out of band noise and improve the signal of interest. It should be noted that all components used in the receive system are carefully characterized by measuring the losses introduced by each component. This will ensure a fair comparison between measurements across different frequency bands.

The antennas utilized for these measurements include short dipoles ($\lambda/5$) and a highly miniaturized antenna ($\lambda/250$), all of which are designed to operate at the lower VHF band. In order to tune the $\lambda/5$ short dipole to the desired center frequency of 40 MHz and enhance its gain, two high-quality factor (Q) coils are utilized on either arm of the short dipole. The system diagram of the 40 MHz measurement is given in Figure 1a.

2.2. Highly Miniaturized Antenna at 40 MHz

A key consideration for establishing a compact, mobile communication system in the lower VHF band is the large size of the antenna owing to the long electrical wavelength at this frequency band. While different types of miniaturized antennas for VHF applications have been reported in the literature [*Zhang et al.*, 2009;

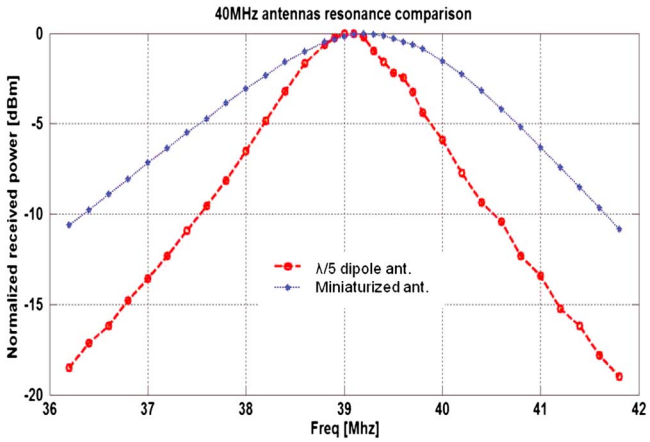

Figure 4. Normalized receive power versus frequency, for two different transmit antennas. Dashed: miniaturized antenna; solid: $\lambda/5$ dipole. The $\lambda/5$ dipole was used on receive for both cases.

Table 1. Comparisons of Parameters Used for 40 MHz and 2.4 GHz Propagation Measurements Carried Out in the Three Scenarios Described in Section 3[a]

	40 MHz	2.4 GHz
P_t (GG Brown)	35 dBm	15 dBm
P_t (EECS)	15 dBm	10 dBm
P_t (ERB)	5 dBm	15 dBm
Tx ant	Small ant	$\lambda/2$ dipole
Rx ant	$\lambda/5$ dipole	$\lambda/2$ dipole
G_{Tx}	−21 dBi	2.15 dBi
G_{Rx}	−0.96 dBi	2.15 dBi
h_{Tx}	1.22 m (0.16λ)	3.2 cm (0.26λ)
h_{Rx}	1.62 m (0.22λ)	3.2 cm (0.26λ)
Tx Rx pol.	V,V	V,V
Rx amp gain	40 dB	30 dB
Imp. mismatch loss	1.5 dB	-
Filter losses	1.5 dB	-
Cable losses	0.3 dB	2.8 dB
Near-ground path loss compensation	-	3.1 dB

[a]Near-ground path loss difference compensation is calculated based on *Liao and Sarabandi* [2005]. EECS: Electrical Engineering and Computer Science Building; ERB: Engineering Research Building.

Moon et al., 2011, 2012], such antennas are bulky and not appropriate for compact, mobile platforms. In order to enable the mentioned applications as well as to facilitate the ease of wave propagation measurements at the lower VHF band, a highly miniaturized, lightweight antenna was designed and fabricated. The lateral dimension and height of the antenna including the ground plane are 60 mm ($\lambda/125$) and 30 mm ($\lambda/250$) at 40 MHz, respectively. The design approach is based on employing two closely spaced short vertical elements producing in-phase radiated fields to significantly improve the radiation efficiency. The two in-phase vertical elements radiate in such a way that the effective height of the antenna is increased without increasing the physical height of the antenna. This gives rise to the enhanced gain of the monopole-based miniaturized antenna compared to a short monopole with the same height.

To achieve the in-phase radiated fields from electric currents flowing on the two vertical elements while minimizing the size of the antenna, a *T* type 180° phase shifter with a capacitive impedance inverter is used [*Oh et al.*, 2013]. However, a lumped capacitor in the phase shifter cannot be used as it causes an out-of-phase conduction current in the capacitor branch which would result in radiation cancelation. For the sake of avoiding this cancelation and achieving the desired 180° phase shift at the same time, the conventional *T* type 180° phase shifter can be modified by replacing the lumped capacitor with an open stub whose capacitance

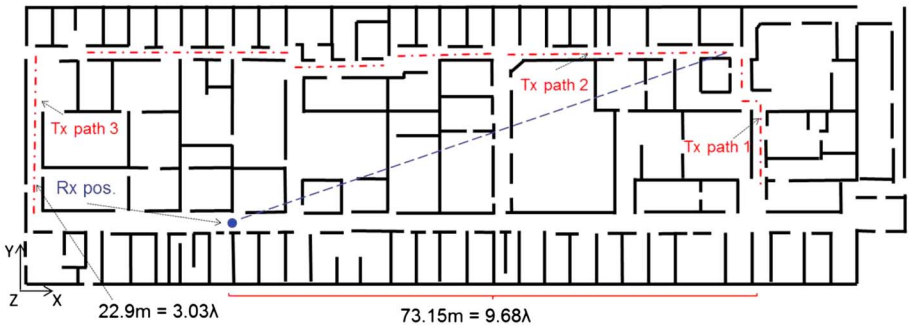

Figure 5. The floor plan of the second floor of the GG Brown building at the University of Michigan. The transmitter paths (Tx paths 1, 2, and 3) are also shown. The receive antenna was positioned at a fixed location (Rx pos.). The dotted diagonal line represents the signal path that penetrates through several layers of walls from the upper right corner of the hallway to the receive antennas.

Table 2. Various Scenarios Considered for Propagation Measurements

	Building	Tx Location	Rx Location	Floor	Setup
Scenario 1	GG Brown	Indoor	Indoor	Second	NLOS
Scenario 2	EECS	Outdoor, Indoor	Indoor	First, Third	NLOS
Scenario 3	ERB	Outdoor	Outdoor	First	NLOS

value is determined by the area of the capacitive loading. The antenna geometry applying the modified *T* type 180° phase shifter is shown in Figure 2. Optimized high *Q* air core inductors (> 1000) are utilized in the phase shifter to minimize power loss from the antenna and integrated between the top and ground plates so as not to increase the overall vertical profile of the antenna. Furthermore, the weight of the antenna is minimized by the use of aluminum wire for construction of the air core inductors and vertical pins. The total measured weight of the fabricated antenna is 18.54 g, which enables integration with small mobile platforms.

Figure 3 shows the 3-D radiation pattern of the antenna tuned to 39.1 MHz. The antenna is vertically polarized and has an omnidirectional radiation pattern as shown in Figure 3. Therefore, it is suitable for near-ground operation since path loss between two near-ground antennas with vertical polarization is far lower than any other polarization [*Liao and Sarabandi*, 2008]. Figure 4 depicts the normalized power received by the $\lambda/5$ dipole antenna, when the miniaturized antenna and an identical $\lambda/5$ dipole antenna are used for transmitter (Tx). The two antennas are tuned to the same operating frequency of 39.1 MHz. The bandwidth of the miniaturized antenna is narrower than that of the $\lambda/5$ dipole antenna due to the high-quality factor of the air core inductors. For this reason, objects that are in close proximity to the antenna ($< \lambda/2\pi$) could impact the performance of the antenna because of a shift in resonance frequency. This effect has been investigated based on measurements, and it has been shown that the resonance frequency is stable in the presence of nearby objects in indoor environments where the distance between the antenna and the object is within the near-field reactive region of the antenna [*Oh et al.*, 2013].

2.3. 2.4 GHz Measurement System

As alluded to earlier, we carry out path loss and small-scale fading measurements at 2.4 GHz in the same scenarios for comparison against the 40 MHz results. A signal generator is used to transmit a 2.4 GHz tone at a power level of 10 dBm. On the receive end, a spectrum analyzer connected to a low-noise amplifier is used to acquire the received signal strength at various locations. Half-wave dipoles are utilized both at the transmitter and receiver for measurements at 2.4 GHz. Relevant parameters of the measurement system are listed in Table 1. Also, a diagram of the measurement system used for the 2.4 GHz measurements is given in Figure 1b.

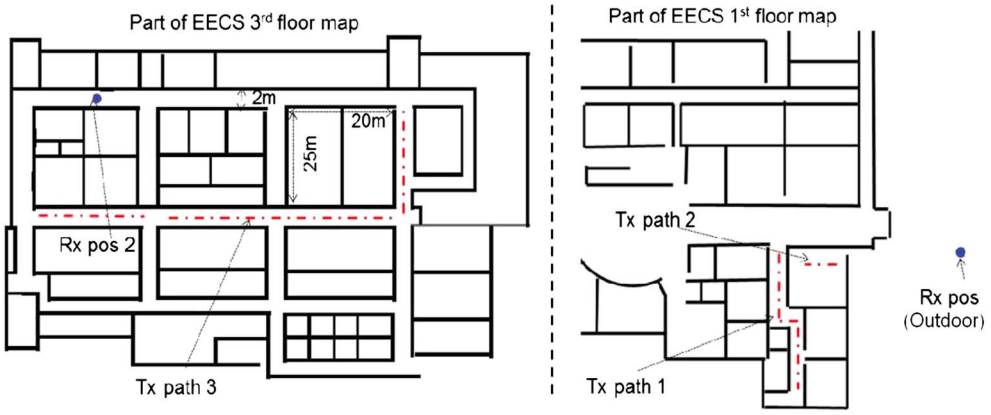

Figure 6. The floor plans of the first and third floors of the Electrical Engineering building at the University of Michigan. The transmitter paths (Tx paths 1, 2, and 3) are also shown. The receive antenna was positioned at two locations (Rx pos. 1 and Rx pos. 2).

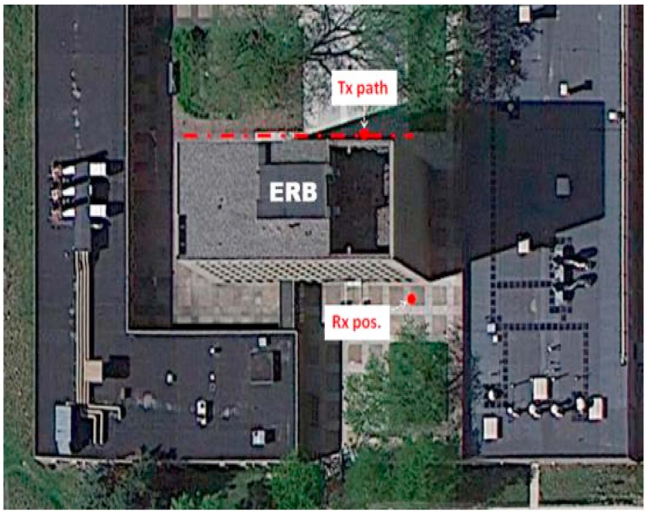

Figure 7. The top view of the Engineering Research Building (ERB) at the University of Michigan. The receive antenna was positioned at Rx pos., and Tx antenna is moved along the Tx path as indicated.

3. Measurement Scenarios

The measurements were collected in three different environments. For all the buildings, the wall thickness varied from 20 to 30 cm. The floor map of the first building where the measurements were carried out is shown in Figure 5. This is a large office building with interior walls made of cinder blocks with metallic reinforcements on the ceiling and floors. It should be noted that many of the rooms in this building contain furniture, including metallic cabinets, tables, and chairs. The transmit and receive antenna arrangements for the measurements obtained in this building are shown in Table 2.

The second building is shown in Figure 6 and has interior walls that are built from bricks, covered by drywalls and metallic studs. The floor and ceilings also include metallic mesh with spacing well below the wavelength in the lower VHF band. It should be noted that the presence of periodic metallic studs in the walls, floors, and ceilings can cause significant attenuation of low-frequency signals including in the lower VHF. This attenuation is even more pronounced for vertical polarization because a significant fraction of the transmitted signal will be reflected by the vertical metallic studs. This building was chosen to study lower VHF propagation and quantify path loss in a challenging scenarios with significant metallic barriers. Both outdoor-to-indoor and indoor-to-indoor links are studied based on measurements carried out in this building.

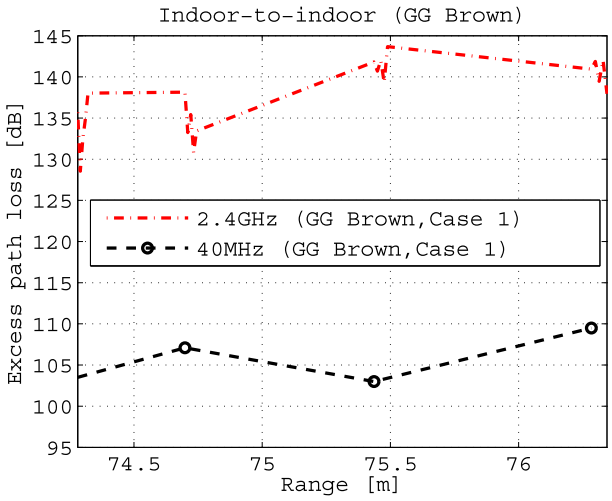

Figure 8. Comparison of path loss at 40 MHz and 2.4 GHz for Case 1 (Tx path 1 and receiver fixed at Rx pos.) of the GG Brown building shown in Figure 5.

In a third scenario, outdoor measurements were conducted adjacent to the building shown in Figure 7. This building is also built from bricks and includes significant metallic reinforcement, and the interior contains office furniture and a variety of metallic objects. This set of measurements is utilized to investigate the

Table 3. Summary of Measurements in Three Different Buildings

	Building	Tx Path	Rx Pos.	Maximum Tx-Rx Distance	Number of Walls Between Tx and Rx	Path Loss Difference (2.4 GHz Versus 40 MHz)
Case 1	1	1	Rx pos.	76 m (~ 10λ)	$\leq$ 14	~35
Case 2	1	2	Rx pos.	45 m (~ 10λ)	$\leq$ 14	~35
Case 3	2	1	1	33 m (~ 4.7λ)	$\leq$ 4	~40
Case 4	2	2	1	23 m (~ 4.7λ)	$\leq$ 4	~45
Case 5	3	1	1	36 m (~ 4.7λ)	$\leq$ 7	~55

path loss in outdoor-to-outdoor NLOS links. By placing the Tx and Rx antennas on opposite sides of the building, penetration through the building in the presence of several layers of walls and other scatterers is measured at 40 MHz and 2.4 GHz. A summary of the measurements carried out in three different building environments is given in Table 3.

4. Analysis and Results

In this section, path loss results based on the various measurements are discussed. Specifically, the propagation mechanisms at the lower VHF band and at the 2.4 GHz band are compared. It should be noted that the goal here is not to study path loss in open environments where it is well established that path loss increases with frequency. Instead, propagation measurements and analysis for LOS and NLOS scenarios are performed to compare the penetration loss through layers of building walls and to compare the level of small-scale fading at the two frequency bands. These effects are critical for short-range penetration and communications in the densely cluttered environments under study.

The variations in antenna performance and near-ground propagation effects that vary with frequency are taken into account to accurately characterize the propagation characteristics as a function of frequency [*Dagefu et al.*, 2013]. For each frequency band, the transmit power and the gains of the amplifiers are adjusted as needed to compensate for differences in antenna gain and other system losses including filter and cable loss. Furthermore, the Tx and Rx antennas are positioned so that they have similar heights in terms of electrical length. The reason for this is to make sure the near-ground propagation effects, which are dominant when the height of the antennas are less than a wavelength, are similar at the two frequency bands [*Liao and Sarabandi*, 2005; *Dagefu et al.*, 2015]. Discussion of path loss calculations from the measured data and the results for various types of channels are presented in the rest of this section.

4.1. Path Loss Calculations

In order to compare the channel path loss, all system parameters at the two frequency bands are carefully taken into account. The path loss in decibels can be calculated as a function of frequency as

$$\mathrm{PL}(f) = P_t(f) - P_r(f) + G_t(f) + G_r(f) + G_{\mathrm{Sys}}(f), \quad (1)$$

where $P_t(f)$ and $P_r(f)$ are the transmit and receive power in decibels, respectively. Here $G_t(f)$ and $G_r(f)$ are the gains of the Tx and Rx antennas, and $G_{\mathrm{Sys}}(f)$ is the sum of all other system gains and losses including amplifier gain, filter, and cable losses. It should be noted that variations in antenna performance along with other effects such as differences in cable losses are carefully measured at the two frequencies so that the channel path loss can be isolated and compared. This is done by

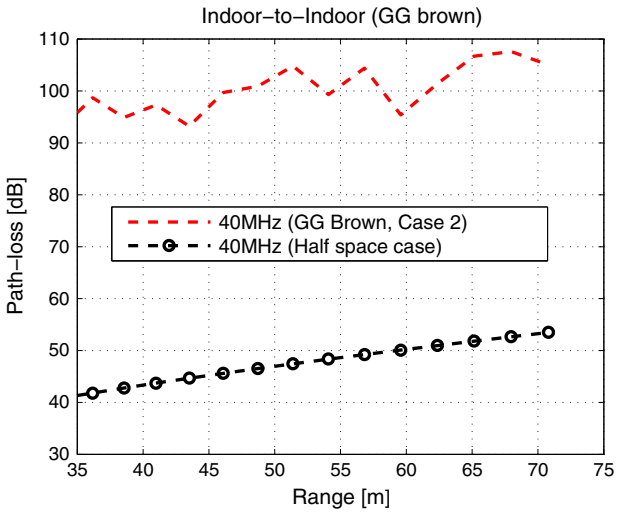

Figure 9. Path loss at 40 MHz for Case 2 (Tx path 2 and receiver fixed at Rx pos.) of the GG Brown building shown in Figure 5.

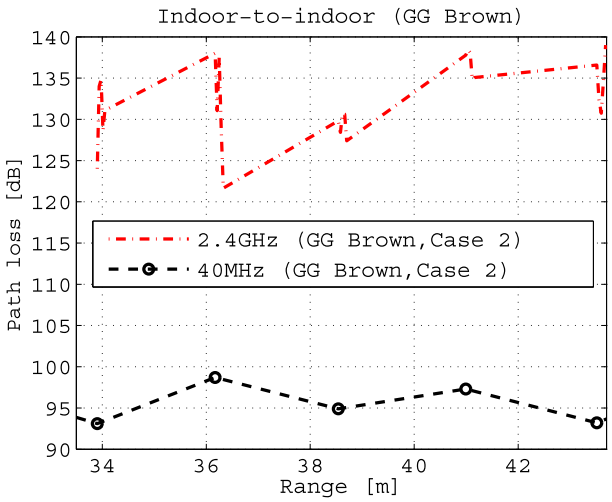

Figure 10. Comparison of path loss at 40 MHz and 2.4 GHz for Case 2 (Tx path 2 and receiver fixed at Rx pos.) of the GG Brown building shown in Figure 5.

making sure that the sum of all gains and the transmit power at each frequency is the same. Appropriate transmit power and amplifier gains are chosen to compensate for differences in antenna gain and other system losses. Table 1 shows a summary of various parameters used for the measurements. It should be noted that the path loss definition given above enables the comparison of signal attenuation and spatial variation induced by the channel based on measured results at the two frequency bands of interest.

4.2. Indoor-to-Indoor Channels

In this section, indoor measurements carried out near 40 MHz and 2.4 GHz are used to quantitatively study the advantages of the lower frequency band for reliable short-range communication in complex propagation scenarios. We are particularly interested in characterizing the NLOS propagation in the lower VHF band where there are many layers of walls and other indoor obstacles between the Tx and Rx antenna. For this scenario, the farthest range between the Tx and Rx antennas is more than 76 m where 14 layers of walls and a multitude of scatterers are located between the Tx and Rx antennas. The received signal in this case consists mainly of the signal that penetrates through the walls, and other diffracted components are much smaller in amplitude. It should be noted that unless the measured point is near a hallway junction, the contribution from diffracted components is quite small.

In order to study path loss in this particular environment, three different NLOS paths are chosen and the measurement results at the lower VHF band (40 MHz) are compared with those obtained from the microwave range (2.4 GHz). The Rx antenna for the measurements is fixed, and the transmitter is moved along different paths (see Figure 5). In both cases, the distance between adjacent transmitter positions is chosen to be less than $\lambda/2$. Comparison between the path loss at the two frequencies of interest for a case where the Tx antenna was moved along Tx path 1 is shown in Figure 8. In Figure 9, the path loss for this indoor scenario is compared against that of the half-space dielectric medium to quantify the loss due to penetration through layers of building walls.

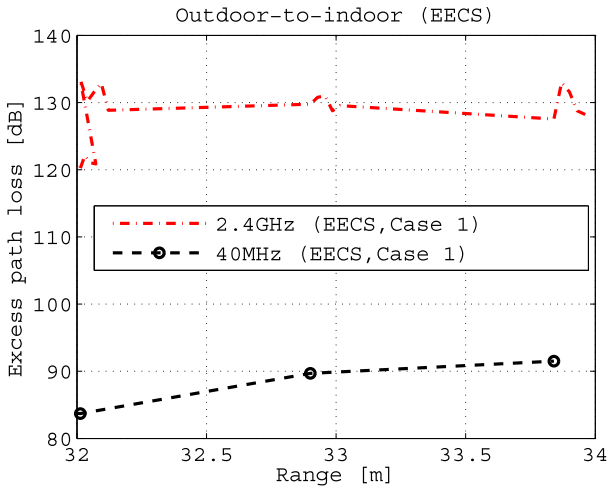

Figure 11. Comparison of path loss at 40 MHz and 2.4 GHz for Case 1 (Tx path 1 and Rx pos.) of the EECS building given in Figure 6.

The path loss comparison for Tx path 2 is given in Figure 10. We note two important points from these results. First, there is significant difference in path loss at 40 MHz and 2.4 GHz. This is because at 40 MHz ($\lambda = 7.5$ m), the thickness of each wall is only a very small fraction of the wavelength, and thus, the signal penetration is significantly better compared to 2.4 GHz ($\lambda = 0.125$ m), where the wall thicknesses are comparable to the wavelength. The second point is the fact that the signal coverage is much smoother at 40 MHz compared to 2.4 GHz where the signal fluctuates quite significantly. This is due to the fact that at the lower VHF band the signal coverage is dominated by the penetrated signal as opposed to reflected

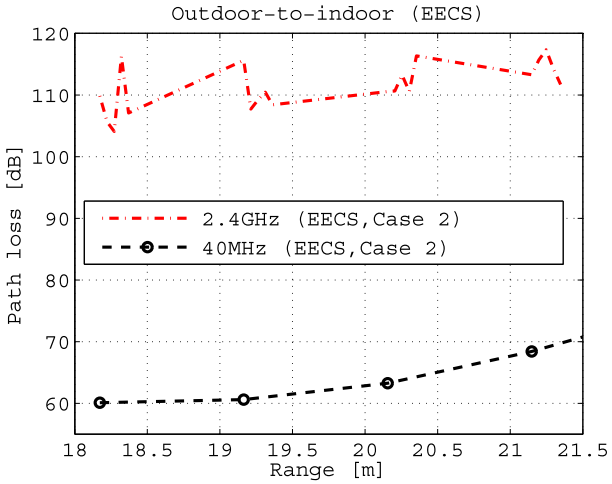

Figure 12. Comparison of excess path loss at 40 MHz and 2.4 GHz for Case 1 (Tx path 1 and Rx pos.) of the EECS building given in Figure 6.

and diffracted components which are dominant at 2.4 GHz.

4.3. Outdoor-to-Indoor and Non-Line-of-Sight Outdoor Channels

Next we consider scenarios where at least one of the antennas is positioned outdoors. The scenarios are shown in Figure 6 where the Rx antenna is positioned outside a building (EECS building at the University of Michigan) and the Tx antenna is moved within the building following different paths. The interior walls of this building have a lot more metallic reinforcement compared to the first building discussed in the previous section. The walls, ceiling, and floor have densely spaced metallic scatterers. We also consider an outdoor-to-outdoor NLOS channel where the two antennas are positioned on either side of a building as depicted in Figure 13. Similar to the previous measurement, the path loss comparison in EECS building for Case 1 (Tx path 1 and Rx at fixed position) and Case 2 (Tx path 2 and Rx at fixed position) are given in Figures 11 and 12, respectively. The path loss comparison for the outdoor-to-outdoor measurement is shown in Figure 13. In each case there is an average of more than 45 dB improvement at 40 MHz compared to 2.4 GHz. Furthermore, the small-scale signal variation is significantly higher at 2.4 GHz which complicates the receiver processing and greatly enhances the probability of intermittent signal dropoff. These effects are minimal at 40 MHz. It should also be noted that the result shown in Figure 13 (outdoor-to-outdoor) shows more signal variation since diffracted components make a more substantial contribution. This is true especially close to the beginning and the end of the Tx path (see Figure 7).

5. Conclusion

In this paper, measurement-based characterization of propagation in the VHF range in cluttered environments is presented. A quantitative path loss comparison between the lower VHF band and the microwave range utilized in conventional systems is carried out. The results point to potential short-range low-power applications of low VHF including reliable short-range communications in highly cluttered environments. In all the measurements at the lower VHF band, a short $\lambda/5$ dipole as well as an extremely small 40 MHz antenna (6 cm by 6 cm by 3 cm) were utilized. A brief discussion of the design and fabrication of the miniaturized antenna was given. Path loss and small-scale fading effects in and around three complex buildings were presented. Propagation scenarios including indoor-to-indoor, outdoor-to-indoor, and NLOS outdoor scenarios are considered, and path loss measurements and signal fading are studied at the lower VHF band (40 MHz) and the microwave band(2.4 GHz). For all scenarios, it is shown that the path loss at 40 MHz is on average 40 dB less than that of the 2.4 GHz case. As discussed earlier, when

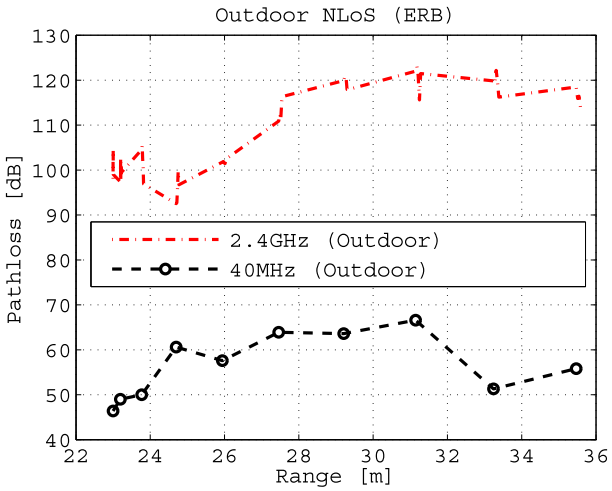

Figure 13. Comparison of path loss at 40 MHz and 2.4 GHz for outdoor-outdoor measurements (Engineering Research Building (ERB) at the University of Michigan given in Figure 7) is shown. The parameters for this measurement are listed in Table 1.

comparing the path loss results, all other variations at the two frequency bands caused by differences in antenna gain, Tx power, and amplifier gains have been accounted for. This was achieved by making sure that the sum of all system attributes affecting the received powers at the two bands (other than the propagation channel) were kept the same. We emphasize that the goal is not to confirm the well-known fact that path loss increases with frequency as in the free space case. The main point of the paper, demonstrated with the measurement results, is that even in highly cluttered environments (in the presence of dielectric and metallic obstacles), the propagation mechanisms at lower VHF and 2.4 GHz are very different. Significant penetration through several layers of building walls is possible at the lower VHF band because of the small electrical size of typical scatterers. On the other hand, at microwave frequencies signal penetration through building walls is small and multipath levels are much more significant. The implication is that the lower VHF band is more suitable for reliable and persistent low-power low-data rate communication in highly cluttered environments. This is true for small platforms using new miniaturized antennas. In addition, the favorable channel characteristics and low signal distortion at the lower VHF enable geolocation and persistent networking, currently under study.

Acknowledgments
The data for this paper can be requested by sending an email to Fikadu Dagefu at fikadu.t.dagefu.ctr@mail.mil. This research was supported in part by National Science Foundation, ECE Program, under Award Number: 1101868 and by the U.S. Army Research Laboratory under contract W911NF-08-2-0004 and prepared through collaborative participation in the Microelectronics Center of Micro Autonomous Systems and Technology (MAST) Collaborative Technology Alliance (CTA).

References

Ali-Rantala, P., L. Ukkonen, L. Sydanheimo, M. Keskilammi, and M. Kivikoski (2003), Different kinds of walls and their effect on the attenuation of radiowaves indoors, in *Antennas and Propagation Society International Symposium, 2003*, vol. 3, pp. 1020–1023, IEEE, Columbus, Ohio.

Andrusenko, J., R. Miller, J. Abrahamson, N. Merheb Emanuelli, R. Pattay, and R. Shuford (2008), VHF general urban path loss model for short range ground-to-ground communications, *IEEE Trans. Antennas Propag.*, *56*(10), 3302–3310, doi:10.1109/TAP.2008.929453.

Choi, J., and K. Sarabandi (2014), Highly miniaturized low-VHF folded dipole antenna for compact, mobile communication applications, *IEEE International Conference on Antennas Propagation*, pp. 2991–2999, Memphis, Tenn., doi:10.1109/TAP.2013.2249034.

Dagefu, F., and K. Sarabandi (2011), Analysis and modeling of near-ground wave propagation in the presence of building walls, *IEEE Trans. Antennas Propag.*, *59*(6), 2368–2378, doi:10.1109/TAP.2011.2144555.

Dagefu, F., J. Oh, and K. Sarabandi (2013), A sub-wavelength RF source tracking system for GPS-denied environments, *IEEE Trans. Antennas Propag.*, *61*(4), 2252–2262, doi:10.1109/TAP.2012.2232036.

Dagefu, F. T., G. Verma, C. R. Rao, P. L. Yu, J. R. Fink, B. M. Sadler, and K. Sarabandi (2015), Short-range Low-VHF channel characterization in cluttered environments, *IEEE Trans. Antennas Propag.*, *63*(6), 1, doi:10.1109/TAP.2015.2418346.

Moon, H., G.-Y. Lee, C.-C. Chen, and J. L. Volakis (2012), An extremely low-profile ferrite-loaded wideband vhf antenna design, *IEEE Antennas Wirel. Propag. Lett.*, *11*, 322–325, doi:10.1109/LAWP.2012.2191131.

Hampton, J. R., N. Merheb, W. Lain, D. Paunil, R. Shuford, and W. Kasch (2006), Urban propagation measurements for ground based communication in the military UHF band, *IEEE Trans. Antennas Propag.*, *54*(2), 644–654, doi:10.1109/TAP.2005.863099.

Holloway, C., P. Perini, R. DeLyser, and K. Allen (1997), Analysis of composite walls and their effects on short-path propagation modeling, *IEEE Trans. Veh. Technol.*, *46*(3), 730–738, doi:10.1109/25.618198.

LaFortune, J.-F., and M. Lecours (1990), Measurement and modeling of propagation losses in a building at 900 MHz, *IEEE Trans. Veh. Technol.*, *39*(2), 101–108, doi:10.1109/25.54226.

Liao, D., and K. Sarabandi (2005), Near-Earth wave propagation characteristics of electric dipole in presence of vegetation or snow layer, *IEEE Trans. Antennas Propag.*, *53*(11), 3747–3756, doi:10.1109/TAP.2005.856347.

Liao, D., and K. Sarabandi (2008), Terminal-to-terminal hybrid full-wave simulation of low-profile, electrically-small, near-ground antennas, *IEEE Trans. Antennas Propag.*, *56*(3), 806–814, doi:10.1109/TAP.2008.916891.

Moon, S.-M., H.-K. Ryu, J.-M. Woo, and H. Ling (2011), Miniaturisation of $\lambda/4$ microstrip antenna using perturbation effect and plate loading for low-VHF band applications, *Electron. Lett.*, *47*(3), 162–164, doi:10.1049/el.2010.3647.

Oh, J., J. Choi, F. Dagefu, and K. Sarabandi (2013), Extremely small two-element monopole antenna for HF band applications, *IEEE Trans. Antennas Propag.*, *61*(6), 2991–2999, doi:10.1109/TAP.2013.2249034.

Pugh, J. A., R. Bultitude, and P. J. Vigneron (2006), Path loss measurements with low antennas for segmented wideband communications at VHF, in *Military Communications Conference, 2006. MILCOM 2006*, pp. 1–5, IEEE, Washington, D. C.

Ruthroff, C. (1971), Multiple-path fading on line-of-sight microwave Radio systems as a function of path length and frequency, *Bell System Tech. J.*, *50*(7), 2375–2398, doi:10.1002/j.1538-7305.1971.tb02612.x.

Zhang, X., T. Burress, K. Albers, and W. Kuhn (2009), Propagation comparisons at VHF and UHF frequencies, in *Radio and Wireless Symposium, 2009. RWS '09*, pp. 244–247, IEEE.